

Optimal Hybrid Macroscopic Traffic Control for Urban Regions: Perimeter and Switching Signal Plans Controllers

Mohammad Hajiahmadi*, Jack Haddad, Bart De Schutter, and Nikolas Geroliminis

Abstract—The dynamics of a heterogeneous large-scale urban network is modeled as R homogeneous regions with the macroscopic fundamental diagrams (MFDs) representations. The MFD provides for homogeneous network regions a unimodal, low-scatter relationship between network vehicle density and network space-mean flow. In this paper, the optimal hybrid control problem for an R -region MFD network is formulated as a mixed integer nonlinear optimization problem, where two types of controllers are introduced: (i) perimeter controllers, and (ii) switching signal timing plans controllers. The perimeter controllers are located on the border between the regions, as they manipulate the transfer flows between them, while the switching controllers control the dynamics of the urban regions, as they define the shape of the MFDs, and as a result affect the internal flows within each region. Moreover, to decrease the computational complexity due to the nonlinear and non-convex nature of the formulated optimization problem, we rewrite the problem as a mixed integer linear problem utilizing a piecewise affine approximation technique. The performance of the two problems is evaluated and compared for different traffic scenarios for a two-region urban case study.

I. INTRODUCTION

Large-scale urban networks need efficient traffic management and control schemes. Modeling a large urban network would be a complex task if one wants to study and model the traffic flow dynamics of each element (i.e. each link and each intersection). Hence, instead of adopting a macro-modeling approach, researchers investigate the possibilities of deriving an aggregate model for the whole traffic network.

Macroscopic fundamental diagrams (MFDs) have been observed for homogeneous urban network regions from empirical and simulation data [1]. The MFD captures (at a network level) the traffic flow characteristics of an urban region. It relates the number of vehicles (accumulation) in the region and its production, defined as the trip completion flow of vehicles. Homogeneous networks with small variance of link densities have a *well-defined* MFD (as illustrated in Fig. 1), i.e. low scatter of flows for the same densities (or accumulations), [2]. Note that the network topology, the signal timing plans of the signalized intersections, and the infrastructure characteristics affect the shape of the MFD, see e.g. [3]. Moreover, heterogeneous networks might not have a well-defined MFD, mainly in the decreasing part of the MFD, and the scatter becomes higher as accumulation increases. As a solution, these networks

This work is partially supported by the European 7th Framework Network of Excellence HYCON2 and the European COST Action TU1102.

Mohammad Hajiahmadi and Bart De Schutter are with the Delft Center for Systems and Control (DCSC), Delft University of Technology.

Jack Haddad and Nikolas Geroliminis are with the Urban Transport Systems Laboratory (LUTS), École Polytechnique Fédérale de Lausanne (EPFL).

* Corresponding author: m.hajiahmadi@tudelft.nl

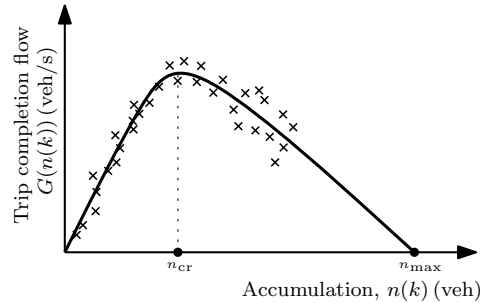


Fig. 1. A well-defined macroscopic fundamental diagram.

might be partitioned into more homogeneous regions with small variances of link densities MFD [4]. Other investigations of the MFD using empirical or simulated data can be found in [5]–[7], while routing strategies based on the MFD can be found in [8].

The MFD can be utilized to establish elegant schemes to decrease delays and increase accessibility in large urban networks. Meanwhile, the idea of focusing the control efforts only on the urban region borders has attracted many researchers, e.g. the perimeter control as in [9]–[11]. The perimeter controllers manipulate the percentage of flows between two regions to maximize the total number of trips completed.

In this paper, we introduce a new type of controller besides the perimeter controllers, that can control the traffic flow dynamics of each urban region by switching between the signal timing plans. Changing timing plans for the signalized intersections within each region might alter the shape of the MFD, which will affect the network flow dynamics. Therefore, instead of assuming one MFD for each region, we introduce a set of MFDs (library), where each MFD corresponds to a certain timing plan for intersections inside the region.

Switching between timing plans together with perimeter control could fulfill the traffic objectives for a vast variety of demands and traffic conditions. However, combining these two control entities is a complex task and not straightforward, as a mixture of discrete and continuous control inputs is introduced in the total nonlinear hybrid model of the network. The model predictive control (MPC) [12] is used to solve the associated optimal control problem. Since we deal with a hybrid system, the resulting optimization problem is a nonlinear mixed integer problem. Solving nonlinear and nonconvex optimization problems can be time consuming and finding a global optimum solution is not guaranteed. As a solution, one can try to approximate and transform the model into a mixed linear form and formulate the optimization problem as a mixed integer linear programming (MILP) problem. The computation time will decrease significantly and one global optimum will exist.

The rest of the paper is organized as follows. In Section II, an MFD-based model of an R -region urban network is derived, while in Section III the optimal hybrid control problem is formulated. A mixed linear dynamic model based on piecewise affine (PWA) approximation of the original model is proposed in Section IV. Performance of the two models is tested for two case study examples with different scenarios in Section V. The paper concludes with a discussion about the results and ideas for further research.

II. MFD-BASED MODELING OF URBAN REGIONS

Let us assume that a heterogeneous network can be partitioned into R homogeneous regions, each having a well-defined MFD (later we assume that each homogeneous region can have a set of different MFDs corresponding to the activated signal timing plans), see Fig. 2. In this paper, the time step and the sample time of the model are denoted by k (–) and T (s), respectively, where $t = k \cdot T$ and $k = 0, 1, 2, \dots, K - 1$. Let $q_{ij}(k)$ (veh/s) be the traffic flow demand generated in region i with direct destination to region j at time step k , $i = 1, 2, \dots, R$, and $j \in \mathcal{S}_i$, where \mathcal{S}_i is the set of regions that are directly reachable from region i . Corresponding to the traffic demands, accumulation states are defined to model the dynamic equations: $n_{ij}(k)$ (veh), where $n_{ij}(k)$ is the total number of vehicles in region i with direct destination to region j at time step k . Let us denote $n_i(k)$ (veh) as the accumulation or the total number of vehicles in region i at time step k , i.e. $n_i(k) = n_{ii}(k) + \sum_{j \in \mathcal{S}_i} n_{ij}(k)$.

The MFD is defined by $G_i(\cdot)$ (veh/s) which is the trip completion flow for region i at $n_i(k)$. The trip completion flow for region i is the sum of transfer flows, i.e. trips from i with destination j , $j \in \mathcal{S}_i$, plus the internal flow, i.e. trips from i with destination i . The *transfer flow* from i with destination to j , denoted by $M_{ij}(k)$ (veh/s), is calculated corresponding to the ratio between accumulations, i.e. $M_{ij}(k) = n_{ij}(k)/n_i(k) \cdot G_i(n_i(k))$, $j \in \mathcal{S}_i$, while $M_{ii}(k)$ is the *internal flow* from i with destination to i and calculated by $M_{ii}(k) = n_{ii}(k)/n_i(k) \cdot G_i(n_i(k))$. These relationships assume that trip length for all trips within a region (internal or external) are similar, i.e. the distance traveled per vehicle inside a region is independent of the origin and destination of the trip. For a description of different cases the reader can refer to [13], which will not alter the methodology. We use a third-order function of $n_i(k)$ to describe the MFD, e.g. $G_i(n_i(k)) = a_i \cdot n_i^3(k) + b_i \cdot n_i^2(k) + c_i \cdot n_i(k)$, where a_i, b_i, c_i are estimated parameters. The mass conservation equations (without integrating control measures) of the R -region MFDs system are as follows:

$$n_{ii}(k+1) = n_{ii}(k) + T \cdot (q_{ii}(k) + \sum_{j \in \mathcal{S}_i} M_{ji}(k) - M_{ii}(k)) \quad (1)$$

$$n_{ij}(k+1) = n_{ij}(k) + T \cdot (q_{ij}(k) - M_{ij}(k)) \quad (2)$$

for $i = 1, 2, \dots, R$ and $\forall j \in \mathcal{S}_i$. These equations are a generalized (R regions instead of two) and discretized form of the continuous-time equations presented in [9]. Note that route choice modeling is not integrated in the dynamic equations.

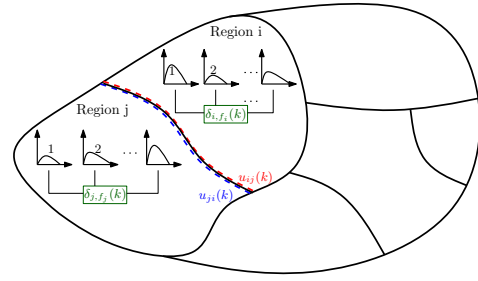


Fig. 2. Hybrid R -region MFDs system with perimeter and switching timing plans control inputs $u_{ij}(k)$ and $\delta_{i,f_i}(k)$ for region i , respectively, and $u_{ji}(k)$ and $\delta_{j,f_j}(k)$ for region j , respectively.

III. OPTIMAL HYBRID CONTROL FOR AN R -REGION MFDs SYSTEM

In the previous section, the MFD-based model (1)-(2) of urban regions was introduced without any control. In the following, two type of controllers are introduced in Section III-A and integrated into the dynamic equations (1) and (2) in Section III-B, while in Section III-C the optimal hybrid control problem for the R -region MFDs system is formulated.

A. Hybrid Control: Perimeter and Switching Controllers

Two types of controllers are introduced in the hybrid control problem: (i) perimeter controllers, and (ii) switching signal timing plans controllers. The perimeter controllers are located on the border between the regions, as they manipulate the *transfer flows* between them, while the switching controllers control the dynamics of the urban regions, as they define the shape of the MFDs, and as a result affect the *internal flows* within each region.

The signal timing plans affect the shape of the MFD, see [3]. In this paper, it is assumed that each urban region has a predefined library of signal fixed-timing plans for the signalized intersections inside the region, e.g. fixed-timing plans for the morning and evening peak hours and a typical uncongested hour, where each plan in the library has different green, red, cycle, and offset settings for the intersections. It is also assumed that for each activated signal plan, the region will have similar shape of MFD, i.e. a non-symmetric unimodal curve skewed to the right, but with different values of the maximum output, and critical and jam accumulations, see e.g. three different MFDs for regions i and j in Fig. 2. Therefore, the timing plan library employs a number of MFDs for the region. The switching controller activates one MFD from the library by switching from one signal plan to another.

The optimal perimeter and switching plans decisions are obtained by minimizing the total delay in the R urban regions. The total delay (veh · s) in the urban regions is defined as follows:

$$J = T \cdot \sum_{k=1}^{K-1} \sum_{i=1}^R n_i(k) \quad (3)$$

B. Hybrid R -Region MFDs System

Let us denote the perimeter control inputs by $u_{ij}(k)$ (–), $i = 1, 2, \dots, R$, $j \in \mathcal{S}_i$, and the switching timing plans control inputs by $\delta_{i,f_i}(k) \in \{0, 1\}$, where $f_i \in \mathcal{F}_i$ and \mathcal{F}_i is the set

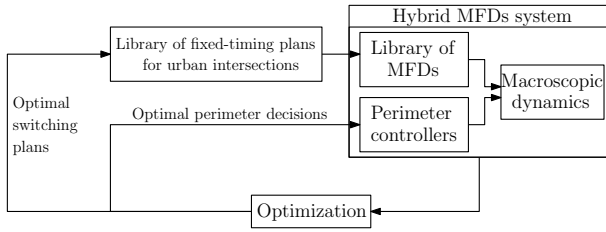


Fig. 3. Optimal hybrid perimeter and switching plans control for urban regions.

of MFDs in the library for region i . The control inputs $u_{ij}(k)$, $\delta_{i,f_i}(k)$, and $u_{ji}(k)$, $\delta_{j,f_j}(k)$ are associated with regions i and j , respectively.

The perimeter controllers $u_{ij}(k)$ and $u_{ji}(k)$ are introduced on the border between the regions i and j as shown in Fig. 2. The transfer flow $M_{ij}(k)$, $i = 1, 2, \dots, R$, $j \in \mathcal{S}_i$, is controlled such that only a fraction of the flow actually transfers from region i to region j , i.e. $u_{ij}(k) \cdot M_{ij}(k)$, where $0 \leq u_{ij}(k) \leq 1$. Hence, the MFD-based model (1) and (2) is altered by replacing $M_{ij}(k)$ and $M_{ji}(k)$ by $u_{ij}(k) \cdot M_{ij}(k)$ and $u_{ji}(k) \cdot M_{ji}(k)$, respectively. It is also assumed that these controllers will not change the shape of the MFDs.

The switching controllers can manipulate indirectly the internal flows by switching the MFDs. Let us now assume that each region i has a predefined MFD library (or set of MFDs denoted by \mathcal{F}_i) that corresponds to a signal timing plans library for the signalized intersections. The switching control signal $\delta_{i,f_i}(k)$ activates the f_i -th MFD in the set \mathcal{F}_i , i.e. $G_{i,f_i}(\cdot)$, if $\delta_{i,f_i}(k) = 1$ and $\delta_{i,r_i}(k) = 0$, $\forall r_i \neq f_i \in \mathcal{F}_i$ (only one $\delta_{i,f_i}(k) = 1$ at any time step, i.e. $\sum_{f_i \in \mathcal{F}_i} \delta_{i,f_i}(k) = 1$). Therefore, the R -region MFDs system (1) and (2) is modified to integrate the switching controllers, as the term $G_i(n_i(k))$ is changed to $\sum_{f_i \in \mathcal{F}_i} \delta_{i,f_i}(k) \cdot G_{i,f_i}(n_i(k))$.

C. Optimal Control Problem Formulation

After introducing and integrating the controllers into the hybrid R -region MFDs system, we formulate the optimal hybrid control problem. The scheme of the optimal control problem is presented in Fig. 3. The aim is to minimize the total delay (3) by manipulating the perimeter controller and switching between the library timing plans.

In reality, homogeneous regions have an MFD with low scatter particularly in the congested regime as shown schematically in Fig. 2. Therefore, errors are expected between the hybrid R -region MFD model (assuming well-defined MFDs) and the real network. Therefore, a closed-loop optimal control scheme is needed in order to take into account the errors between the plant and the model and also the disturbances, e.g. variations in the expected demands. Among these schemes is the model predictive control (MPC) framework, which has been widely used for different traffic control purposes [14]–[17]. The MPC determines the optimal control inputs in a receding horizon manner, meaning that at each time step an objective function is optimized over a prediction horizon of N_p and a sequence of optimal control inputs are derived. Then the first sample of the control inputs is applied to the system and the procedure is carried out again with a shifted horizon.

We directly formulate the problem in the form of the model predictive control. Let k_c (–) and T_c (s) be the control time step counter and its length. It is assumed that the controller time step length is an integer multiple of the model time step length, i.e. $T_c = M \cdot T$. Then, the overall optimization problem is formulated as follows:

$$J(k_c) = \min_{\tilde{u}_{ij}(k_c), \tilde{\delta}_{i,f_i}(k_c)} T \cdot \sum_{k=M \cdot k_c}^{M \cdot (k_c + N_p) - 1} \sum_{i=1}^R n_i(k) \quad (4)$$

subject to:

$$n_{ii}(k+1) = n_{ii}(k) + T \cdot (q_{ii}(k) + \sum_{j \in \mathcal{S}_i} u_{ji}(k) \cdot M_{ji}(k) - M_{ii}(k)) \quad (5)$$

$$n_{ij}(k+1) = n_{ij}(k) + T \cdot (q_{ij}(k) - u_{ij}(k) \cdot M_{ij}(k)) \quad (6)$$

$$M_{ii}(k) = \frac{n_{ii}(k)}{n_i(k)} \cdot \left[\sum_{f_i \in \mathcal{F}_i} \delta_{i,f_i}(k) \cdot G_{i,f_i}(n_i(k)) \right] \quad (7)$$

$$M_{ij}(k) = \frac{n_{ij}(k)}{n_i(k)} \cdot \left[\sum_{f_i \in \mathcal{F}_i} \delta_{i,f_i}(k) \cdot G_{i,f_i}(n_i(k)) \right] \quad (8)$$

$$n_i(k) = n_{ii}(k) + \sum_{j \in \mathcal{S}_i} n_{ij}(k) \quad (9)$$

$$0 \leq n_i(k) \leq n_{i,\text{jam}} \quad (10)$$

$$u_{ij,\text{min}} \leq u_{ij}(k) \leq u_{ij,\text{max}} \quad (11)$$

$$u_{ij}(k) = u_{ij}^c(k_c) \text{ if } k \in \{M \cdot k_c, \dots, M \cdot (k_c + 1) - 1\} \quad (12)$$

$$\delta_{i,f_i}(k) = \delta_{i,f_i}^c(k_c) \text{ if } k \in \{M \cdot k_c, \dots, M \cdot (k_c + 1) - 1\} \quad (13)$$

$$\delta_{i,f_i}(k) \in \{0, 1\}, \forall f_i \in \mathcal{F}_i \quad (14)$$

for $i = 1, 2, \dots, R$ and $\forall j \in \mathcal{S}_i$, where $n_{i,\text{jam}}$ (veh) is the jam accumulation for region i , and $u_{ij,\text{min}}$ and $u_{ij,\text{max}}$ (–) are respectively the lower and upper bounds for the perimeter controllers for regions i and j . The optimization variables defined over the prediction horizon N_p are $\tilde{u}_{ij}(k_c) = [u_{ij}^c(k_c), \dots, u_{ij}^c(k_c + N_p - 1)]$ and $\tilde{\delta}_{i,f_i}(k_c) = [\delta_{i,f_i}^c(k_c), \dots, \delta_{i,f_i}^c(k_c + N_p - 1)]$, where $u_{ij}^c(k_c + l)$ and $\delta_{i,f_i}^c(k_c + l)$ for $l = 0, \dots, N_p - 1$ are the perimeter and switching control inputs at every control time step k_c , respectively.

The problem (4)–(14) is a mixed integer nonlinear optimization problem (MINLP) and can be solved using mixed integer nonlinear optimization algorithms [18]. However, due to the fact that here we deal with both real and binary decision variables and also since the model equations have nonlinear terms, the optimization problem could have multiple (local) optimal points. Moreover, as will be demonstrated in Section V, the optimization algorithm takes considerable time, specially due to the fact that the algorithm should be executed for several random initial points in order to prevent reaching local optima only. Thus, in the next section we simplify and reformulate the problem in order to eventually establish a mixed integer *linear* optimization problem.

IV. APPROXIMATION OF THE R -REGION MFDs SYSTEM

In this section, we aim at recasting the problem into a mixed integer *linear* optimization problem. The nonlinear model in

the MPC framework (4)–(14) is replaced by an approximated model following a piecewise affine (PWA) approximation. The idea of PWA approximation of MFDs was presented in a hierarchical control framework for intelligent vehicle highway systems in [19]. The nonlinearity in the dynamic equations is present in: (i) the internal and transfer trip completion flows, see $M_{ii}(k)$ in (7) and $M_{ij}(k)$ in (8), respectively, and (ii) the product between the perimeter controllers and the transfer trip completion flows, see (5) and (6). In the following, we address these nonlinearities and obtain the PWA approximations.

A. PWA Approximation of the Trip Completion Flows

The nonlinearity in the internal trip completion flows $M_{ii}(k)$ is approximated as follows (a similar procedure is applied to the transfer trip completion flows $M_{ij}(k)$). Substituting the third-order function $G_{i,f_i}(n_i(k)) = a_{i,f_i} \cdot n_i^3(k) + b_{i,f_i} \cdot n_i^2(k) + c_{i,f_i} \cdot n_i(k)$ into (7), one can re-write the internal flows $M_{ii}(k)$ for $i = 1, 2, \dots, R$ as follows:

$$M_{ii}(k) = n_{ii}(k) \cdot \left[\sum_{f_i \in \mathcal{F}_i} \delta_{i,f_i}(k) \cdot (a_{i,f_i} \cdot n_i^2(k) + b_{i,f_i} \cdot n_i(k) + c_{i,f_i}) \right]. \quad (15)$$

The function $P_{i,f_i}(n_i(k)) = a_{i,f_i} \cdot n_i^2(k) + b_{i,f_i} \cdot n_i(k) + c_{i,f_i}$ (inside the parentheses in (15)) defined on the interval $[n_{i,\min}, n_{i,\max}]$ can be approximated by a continuous PWA function $\hat{P}_{i,f_i}(n_i(k))$ with two intervals as follows:

$$\hat{P}_{i,f_i}(n_i(k)) = \begin{cases} \gamma_{i,f_i} + \frac{n_i(k) - n_{i,\min}}{\alpha_{i,f_i} - n_{i,\min}} \cdot (\xi_{i,f_i} - \gamma_{i,f_i}) & \text{for } n_{i,\min} \leq n_i(k) < \alpha_{i,f_i}, \\ \xi_{i,f_i} + \frac{n_i(k) - \alpha_{i,f_i}}{n_{i,\max} - \alpha_{i,f_i}} \cdot (\epsilon_{i,f_i} - \xi_{i,f_i}) & \text{for } \alpha_{i,f_i} \leq n_i(k) < n_{i,\max}. \end{cases} \quad (16)$$

where the parameters γ_{i,f_i} , α_{i,f_i} , ξ_{i,f_i} , and ϵ_{i,f_i} can be estimated using different methods, e.g. a nonlinear least-squares method [20].

However, the multiplication of $n_{ii}(k)$ with the other variables in the square brackets in (15), results in multiple products of variables. In principle, each product needs to be approximated by a PWA function (holds also for $n_{ij}(k)$). This makes the approximation a tedious task as more parameters have to be introduced (see e.g. [21]). Hence, in order to simplify the approximation, we estimate the variables $n_{ii}(k)$ and $n_{ij}(k)$ as follows: we first simulate the R -region MFDs system according to the model presented in (5)–(6) over a prediction horizon with control inputs and initial accumulations obtained from the previous time step, and subsequently the variables $n_{ii}(k)$ and $n_{ij}(k)$ in $M_{ii}(k)$ and $M_{ij}(k)$ are replaced with the values obtained from the simulation. Hence, we no longer deal with multiplication of variables but only with multiplication with time-varying but known parameters.

B. PWA Approximation of the Product between the Perimeter Controllers and the Transfer Flows

The transfer flows are multiplied with the perimeter controller inputs in (5) and (6). These products are not replaced

with values obtained from simulation. Instead, one can assume that the control inputs $u_{ij}(k)$ are quantized as follows [22]:

$$u_{ij}(k) = u_{ij,0} \cdot \left(\sum_{l=0}^r 2^l \cdot \omega_{ij,l}(k) \right) \quad (17)$$

where $\omega_{ij,l}(k) \in \{0, 1\}$ and $u_{ij,0}$ are constant. The set of possible input values is finite and its cardinality is 2^{r+1} , while the difference between two consecutive values is determined by $u_{ij,0}$. Having a sum of weighted binary variables for each perimeter control input, the problem with multiplication of control inputs with transfer flow functions will be simplified, since multiplication with binaries can be easily handled with the techniques presented in the next section.

C. From PWA to MILP

Since direct integration of the approximated model in the MPC framework is computationally inefficient even for small-sized problems, we make a conversion of the derived model. To this aim, we introduce the following transformation rules from [22]. Consider an affine function $f(\cdot)$ over a bounded set X of the input variable x , with upper and lower bounds M and m over X . Having a binary decision variable $\delta \in \{0, 1\}$, it can be proved that the following statements hold:

- $[f(x) \leq 0] \Leftrightarrow [\delta = 1]$, iff $\begin{cases} f(x) \leq M \cdot (1 - \delta) \\ f(x) \geq \epsilon + (m - \epsilon) \cdot \delta \end{cases}$
- $\delta = \delta_1 \cdot \delta_2$, iff $\begin{cases} -\delta_1 + \delta \leq 0 \\ -\delta_2 + \delta \leq 0 \\ \delta_1 + \delta_2 - \delta \leq 1 \end{cases}$
- $z = \delta \cdot f(x)$, iff $\begin{cases} z \leq M \cdot \delta, & z \geq m \cdot \delta \\ z \leq f(x) - m \cdot (1 - \delta) \\ z \geq f(x) - M \cdot (1 - \delta) \end{cases}$

with ϵ is a small tolerance used to change a strict inequality into a non-strict inequality. Using the above mentioned rules, the approximated model can be transformed into a system of linear inequalities and equations with real and binary variables. Furthermore, integrating this model into the MPC framework with the linear objective function (4), one can formulate a mixed integer linear optimization problem (MILP) that can be solved using efficient solvers [23].

V. CASE STUDY EXAMPLES

In this section, the performance of the proposed hybrid control schemes is evaluated for an urban network that is partitioned into two regions, i.e. $R = 2$, the periphery (region 1) and the city center (region 2). In Example 1, we investigate the performance of the perimeter and switching timing plans control and we show that additional improvements are obtained if both control inputs are considered in the optimization. In Example 2, the performance of the proposed linear approximation is compared with the original nonlinear approach.

A. Example 1

For each region, a set of MFDs is defined. As depicted in Fig. 4(b), the set consists of $MFD_{1,3}$ adopted from [1] and 4 other MFDs obtained based on deviation from the critical accumulation and the maximum trip completion flow of $MFD_{1,3}$.

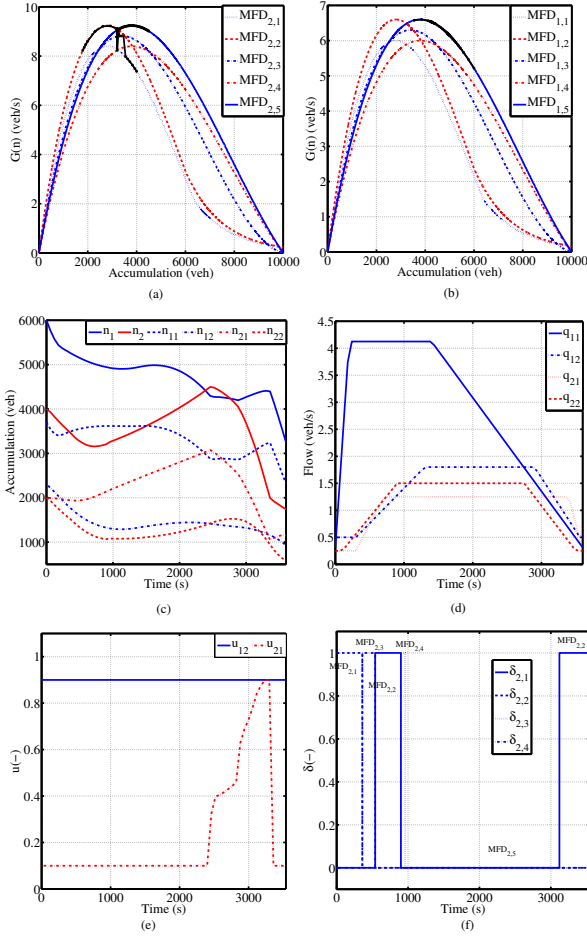


Fig. 4. Example 1: Performance overview of the nonlinear hybrid scheme for a two-region urban network.

The percentages of the deviations are $\pm 10\%$ and $\pm 5\%$ for the critical accumulation and maximum trip completion flow, respectively. Moreover, we assumed that the sizes of the two regions are different, hence the MFDs of the periphery are multiplied by a coefficient as shown in Fig. 4(a) and (b).

The demand profiles for trips inside each region and between them are illustrated in Fig. 4(d). There is a high demand for trips inside the periphery. Further, both regions are initially congested. The hybrid controller finds the optimal perimeter control inputs along with the optimal timing plan, as shown in Fig. 4(e) and (f), for each region using mixed integer nonlinear optimization over the prediction horizon $N_p = 20$ and the control horizon $N_c = 2$. Note that the current choice for these parameters are based on the tuning procedure in [9]. Moreover, the network (reality) is assumed to include errors in the MFDs according to the error formulation in [9]. In the absence of control or having only the perimeter control, region(s) will end up in a gridlock situation. But with optimal switching between timing plans and assisting with perimeter control, both regions will escape from high congestion and they will be eventually uncongested, as in Fig. 4(c).

B. Example 2

In this example, we provide a scenario to evaluate the performance of the proposed approximated model and the original

MINLP formulation in the MPC framework. Moreover, in order to have a better picture, the results are also compared with a greedy perimeter controller, i.e. a simple state-feedback controller. The control laws of the greedy controller are as follows: if both regions are uncongested, the perimeter control inputs are maximized and if both regions are congested, the perimeter control inputs $u_{i,j}$ and $u_{j,i}$ are respectively set to the maximum and minimum values, if region j is more congested than region i and vice versa.

In example 2, each region has a set of 3 MFDs (the same MFD_{1,2}, MFD_{1,3}, and MFD_{1,4} in Fig. 4(b)). The demand profile simulates a peak morning hour with high demand $q_{12}(k)$ for trips from region 1 (the periphery) to region 2 (the city center), as shown in Fig. 5(d). The evolution of accumulations over time corresponding to MINLP and PWA-MILP approaches are depicted in Fig. 5(a) and (b), respectively. These figures demonstrate the effectiveness of the control measures as they show that the control inputs prevent the two regions from moving towards gridlock, which is the case in the absence of any control. However, the nonlinear optimization results in a better performance, in particular for accumulations of region 2. The performance of the PWA-MILP can be further improved by approximation of the polynomials with a larger number of affine functions. Nevertheless, the performance of the PWA-MILP is already much better compared to the greedy controller. With the greedy controller, the accumulations of both regions will exceed 7000 vehicles at the end of the simulation time.

The optimal perimeter control inputs for the nonlinear optimization and PWA-MILP are shown in Fig. 5(c). The perimeter inputs $u_{12}(k)$ of the MINLP algorithm are close to the maximum to allow more vehicles to leave region 1 while $u_{21}(k)$ varies more over time. Moreover, the optimal switching timing plans for the nonlinear and PWA-MILP problems are illustrated in Fig. 5(e) for region 1 and (g) for region 2 and Fig. 5(f) for region 1 and (h) for region 2, respectively.

The average computation time for the current scenario is 13.05 (s) for one run of the MILP algorithm, while it is 51.52 (s) for one run of the MINLP¹. Note that the MINLP has been executed 10 times in each control time step for different random initial points in order to prevent reaching local optimal solution. Therefore, the actual computation time of the MINLP is multiple of the aforementioned number.

VI. CONCLUSIONS

The optimal hybrid perimeter and switching timing plans control for large scale urban networks has been formulated utilizing MFD-based modeling. The optimal solutions were obtained in a model predictive control scheme for two different open-loop optimization problems; mixed integer nonlinear and linear programming. The mixed integer linear programming (MILP) problem was obtained after approximation of the nonlinear model by piecewise affine functions. The obtained results showed the importance of the approximation approach regarding the computational complexity for real-time implementation

¹These CPU times were obtained adopting the functions minlpBB and CPLEX inside the *Tomlab* toolbox of Matlab 7.12.0 (R2011a), on a 64-bit Windows PC with a 2.8GHz Intel Core i7 processor and 8Gb RAM.

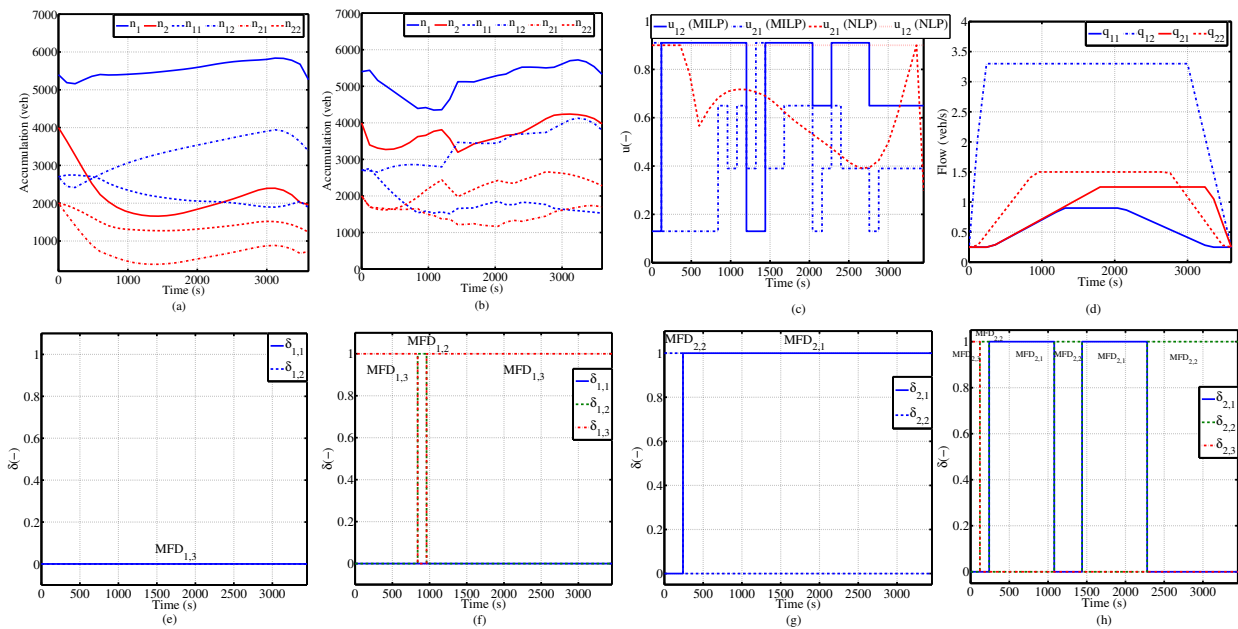


Fig. 5. Example 2: Comparison of PWA-MILP and MINLP for a two-region urban network.

in large-scale networks with large number of regions, as the original nonlinear problem might not be tractable.

The switching timing plans controllers can enhance the network performance when they collaborate with the perimeter controllers, as they can utilize more efficiently the network capacity to decrease the total delay in the network. However, we need to identify the traffic situations in which the hybrid control performs much better than perimeter control only. Furthermore, investigation of other approximation methods that might improve the computation time of the MILP problem is included in the future research.

REFERENCES

- [1] N. Geroliminis and C. F. Daganzo, "Existence of urban-scale macroscopic fundamental diagrams: some experimental findings," *Transportation Research Part B*, vol. 42, no. 9, pp. 759–770, 2008.
- [2] N. Geroliminis and J. Sun, "Properties of a well-defined macroscopic fundamental diagram for urban traffic," *Transportation Research Part B*, vol. 45, no. 3, pp. 605–617, 2011.
- [3] N. Geroliminis and B. Boyaci, "The effect of variability of urban systems characteristics in the network capacity," *Transportation Research Part B*, vol. 46, no. 10, 2012.
- [4] Y. Ji and N. Geroliminis, "On the spatial partitioning of urban transportation networks," *Transportation Research Part B*, vol. 46, no. 10, 2012.
- [5] C. F. Daganzo, V. V. Gayah, and E. J. Gonzales, "Macroscopic relations of urban traffic variables: Bifurcations, multivaluedness and instability," *Transportation Research Part B*, vol. 45, no. 1, pp. 278–288, 2011.
- [6] C. Buisson and C. Ladier, "Exploring the impact of homogeneity of traffic measurements on the existence of macroscopic fundamental diagrams," *Transportation Research Record*, vol. 2124, pp. 127–136, 2009.
- [7] M. Saberli and H. Mahmassani, "Exploring properties of network-wide flow-density relations in a freeway network," in *Transportation Research Board Annual Meeting*, Washington, D.C., 2012.
- [8] V. L. Knoop, S. Hoogendoorn, and J. W. C. Van Lint, "Routing strategies based on the macroscopic fundamental diagram," in *Transportation Research Board Annual Meeting*, Washington, D.C., 2012.
- [9] N. Geroliminis, J. Haddad, and M. Ramezani, "Optimal perimeter control for two urban regions with macroscopic fundamental diagrams: A model predictive approach," *IEEE Transactions on Intelligent Transportation Systems*, vol. 14, no. 1, 2013.
- [10] J. Haddad and N. Geroliminis, "On the stability of traffic perimeter control in two-region urban cities," *Transportation Research Part B*, vol. 46, no. 1, pp. 1159–1176, 2012.
- [11] M. Ramezani, J. Haddad, and N. Geroliminis, "Macroscopic traffic control of a mixed urban and freeway network," in *Proceedings of the 13th IFAC Symposium on Control in Transportation Systems*, 2012, pp. 89–94.
- [12] J. Maciejowski, *Predictive Control with Constraints*. Harlow, England: Prentice Hall, 2002.
- [13] N. Geroliminis, "Dynamics of peak hour and effect of parking for congested cities," in *Transportation Research Board Annual Meeting*, no. 09-1685, Washington, D.C., 2009.
- [14] T. Bellemans, B. De Schutter, and B. D. Moor, "Model predictive control for ramp metering of motorway traffic: A case study," *Control Engineering Practice*, vol. 14, pp. 757–767, 2006.
- [15] I. Papamichail, A. Kotsialos, I. Margonis, and M. Papageorgiou, "Coordinated ramp metering for freeway networks – a model-predictive hierarchical control approach," *Transportation Research Part C*, vol. 18, pp. 311–331, 2010.
- [16] K. Aboudolas, M. Papageorgiou, A. Kouvelas, and E. Kosmatopoulos, "A rolling-horizon quadratic-programming approach to the signal control problem in large-scale congested urban road networks," *Transportation Research Part C*, vol. 18, pp. 680–694, 2010.
- [17] S. Lin, B. De Schutter, Y. Xi, and H. Hellendoorn, "Fast model predictive control for urban road networks via MILP," *IEEE Transactions on Intelligent Transportation Systems*, vol. 12, no. 3, pp. 846–856, 2011.
- [18] B. Borchers and J. E. Mitchell, "A computational comparison of branch and bound and outer approximation algorithms for 0-1 mixed integer nonlinear programs," *Computers and Operations Research*, vol. 24, pp. 699–701, 1996.
- [19] L. Baskar, B. De Schutter, and J. Hellendoorn, "Hierarchical model-based predictive control for intelligent vehicle highway systems: Regional controllers," in *Proceedings of the 13th International IEEE Conference on Intelligent Transportation Systems (ITSC 2010)*, Madeira Island, Portugal, 2010, pp. 249–254.
- [20] R. Fletcher, *Practical Methods of Optimization, Volume 1: Unconstrained Optimization*. Chichester, UK: John Wiley and Sons, 1980.
- [21] G. Ferrari-Trecate, M. Muselli, D. Liberati, and M. Morari, "A clustering technique for the identification of piecewise affine systems," *Automatica*, vol. 39, no. 2, pp. 205–217, 2003.
- [22] A. Bemporad and M. Morari, "Control of systems integrating logic, dynamics, and constraints," *Automatica*, vol. 35, no. 3, pp. 407–427, 1999.
- [23] A. Atamtürk and M. W. P. Savelsbergh, "Integer-programming software systems," *Annals OR*, vol. 140, no. 1, pp. 67–124, 2005.